Highly resolved data set on different phytoplankton pigments retrieved from underway spectrophotometry in the Fram Strait, Arctic Ocean

Yangyang Liu[1,2,*], Emmanuel Boss[4], Alison Chase[4], Yanqun Pan[5], Hongyan Xi[1], Eva-Maria Nöthig[1], Sonja Wiegmann[1], and Astrid Bracher[1,3]

[1]*Alfred Wegener Institute Helmholtz Centre for Polar and Marine Research, Bremerhaven, Germany*
[2]*Institute of Biology and Chemistry, University of Bremen, Bremen Germany*
[3]*Institute of Environmental Physics (IUP), University of Bremen, Bremen, Germany*
[4]*University of Maine, Orono, ME, USA*
[5]*State Key Laboratory of Estuarine and Coastal Research, East China Normal University, Shanghai, China*

Introduction

- Light absorption properties of marine phytoplankton influence the solar radiation into the ocean and control the light energy usable for photosynthesis.
- The shape and magnitude of the phytoplankton absorption spectra is controlled primarily by the concentration of various pigments and the level of package effect within the cells.
- In this study, four approaches to estimate phytoplankton pigment concentration from particulate absorption spectra derived from underway AC-S flow-through system, namely **Gaussian decomposition, singular value decomposition, neural network and empirical orthogonal function analyses**, are evaluated and intercompared.

Data and Method

Cruises tracks with *R.V. Polarstern*

PS 93.2: Jul.-Aug. 2015, Svalbard – Fram Strait
PS 99.2: Jun.-Jul. 2016, Svalbard – Fram Strait
PS 107: Jun.-Jul. 2017, Svalbard – Fram Strait

Data

1 Discrete water sampling every 3h
- PS 93.2: a_p&a_{ph} (high performance spectrophotometer), Chl-a (HPLC)
- PS 99.2 & PS107: a_p&a_{ph} (QFT-ICAM), Chl-a (HPLC)

2 Underway AC-S measurements
- Particulate absorption spectra

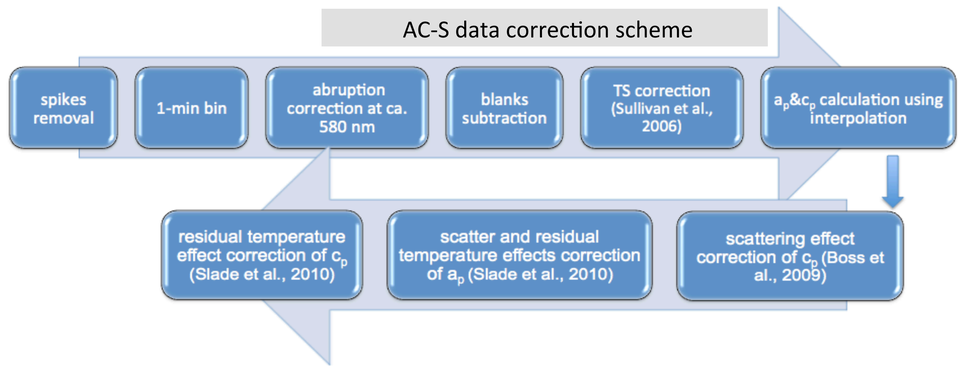

Gaussian Decomposition

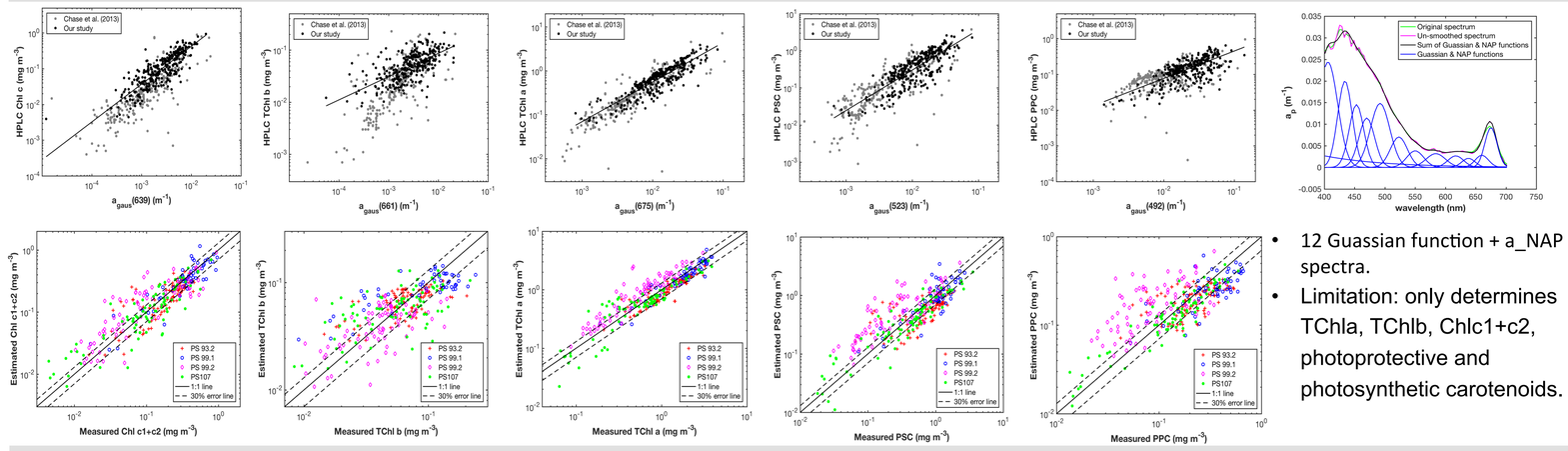

- 12 Guassian function + a_NAP spectra.
- Limitation: only determines TChla, TChlb, Chlc1+c2, photoprotective and photosynthetic carotenoids.

Statistics for Gaussian Decomposition

Pigments	*S*	*I*	*r (log10)*	*RMSE (log10)*	*MAE (log10)*	*Bias (log10)*
TChl a	1.20±0.04	-0.14±0.04	0.89	0.161	0.132	0.011
TChl b	2.25±0.17	-0.06±0.01	0.65	0.201	0.156	-0.001
Chlc_1+2	1.28±0.05	-0.02±0.01	0.84	0.258	0.200	0.005
PSC	1.37±0.06	-0.13±0.04	0.81	0.265	0.216	0.016
PPC	1.73±0.13	-0.11±0.02	0.68	0.238	0.186	0.022

Singular Value Decomposition + Non-Negative Least Square

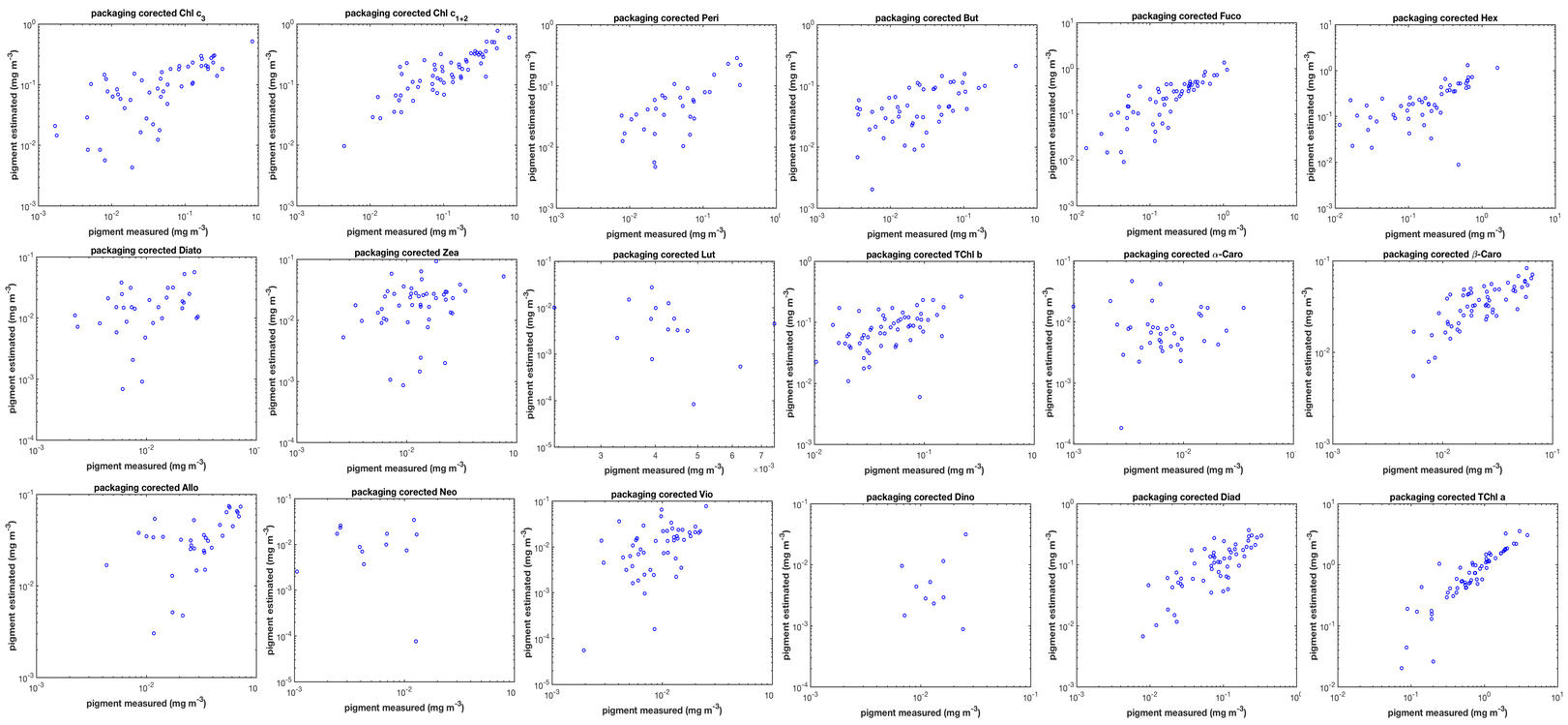

Statistics for SVD-NNLS

Pigments	*S*	*I*	*r (log10)*	*RMSE (log10)*	*MAE (log10)*	*Bias (log10)*
TChl a	0.99±0.05	0.03±0.06	0.89	1.243	1.141	-1.141
TChl b	1.82±0.34	-0.02±0.02	0.46	1.444	1.420	-1.420
Chlc_1+2	0.91±0.07	0.05±0.02	0.85	1.260	1.199	-1.198
Chl_c3	0.72±0.06	0.06±0.01	0.69	1.601	1.505	-1.505
Peri	0.71±0.08	0.01±0.01	0.67	1.490	1.432	-1.432
But	0.44±0.07	0.04±0.01	0.55	1.745	1.678	-1.678
Fuco	1.07±0.07	0.03±0.02	0.81	1.128	1.091	-1.091
Hex	0.93±0.09	0.03±0.03	0.63	1.147	1.082	-1.082
Vio	5.43±1.48	-0.04±0.02	0.50	2.076	2.062	-2.062
Diad	1.13±0.12	0.01±0.02	0.78	1.304	1.258	-1.258
Allo	1.03±0.18	0.00±0.01	0.49	1.616	1.591	-1.591
Dlato	3.00±1.26	-0.02±0.02	0.32	2.044	2.022	-2.022
Zea	3.02±1.32	-0.02±0.02	0.27	1.953	1.934	-1.934
Lut	-17.6±13.0	0.08±0.06	-0.37	2.382	2.380	-2.380
a_Caro	119±3133	-1.00±26.4	0.08	2.218	2.196	-2.196
B_Caro	1.02±0.11	0.01±0.00	0.78	1.717	1.697	-1.697
Neo	26.0±97.4	-0.15±0.62	-0.15	2.336	2.314	-2.314
Dino	1.87±1.01	-0.02±0.01	0.15	1.905	1.896	-1.896

Neural Network

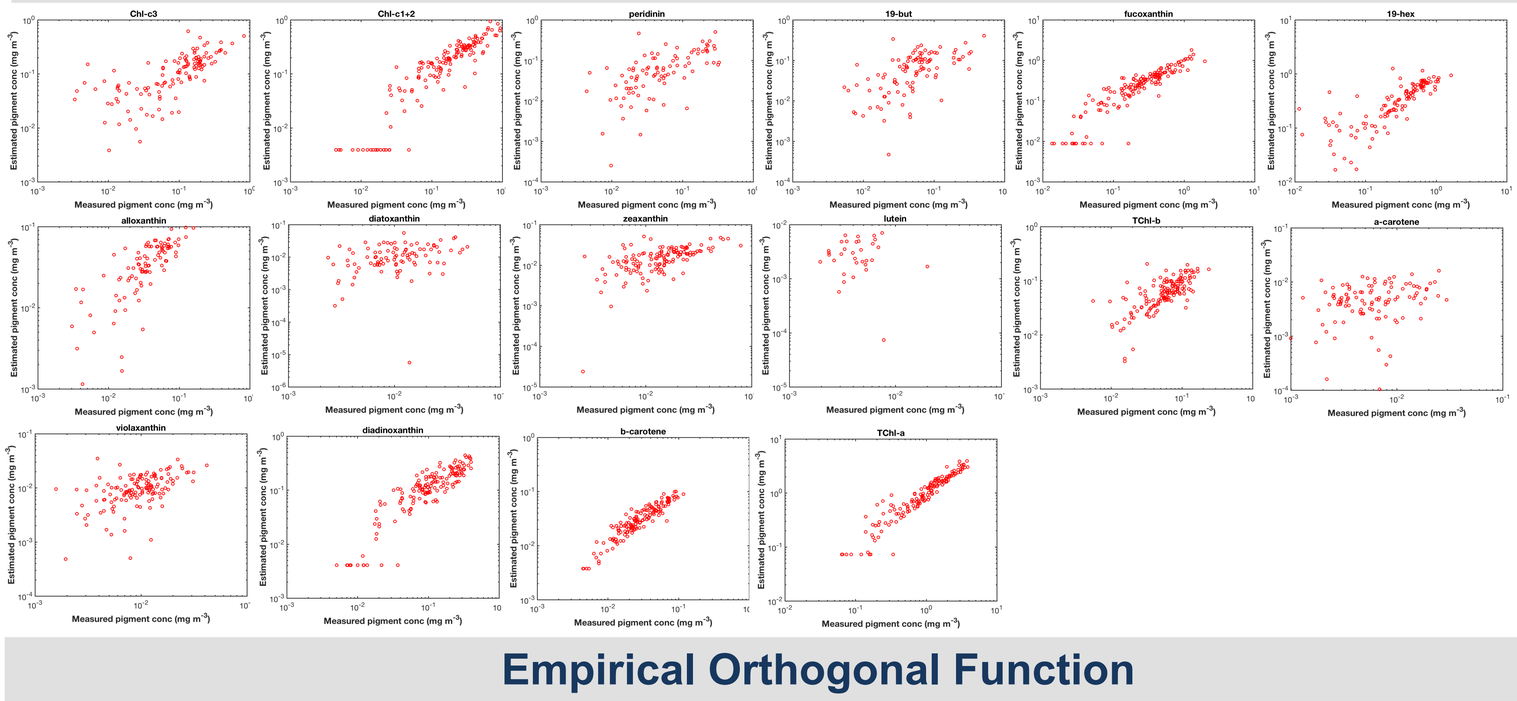

Statistics for NN

Pigments	*S*	*I*	*r (log10)*	*RMSE (log10)*	*MAE (log10)*	*Bias (log10)*
TChl a	0.92	0.06	0.96	0.248	0.175	-0.003
TChl b	0.75	0.02	0.69	0.032	0.022	0.003
Chlc_1+2	0.95	0.01	0.90	0.089	0.055	-0.009
Chl_c3	0.67	0.02	0.78	0.078	0.047	0.001
Peri	0.85	0.00	0.66	0.065	0.034	0.003
But	0.75	0.01	0.67	0.059	0.036	0.001
Fuco	0.97	0.02	0.90	0.138	0.078	-0.000
Hex	0.97	0.00	0.85	0.163	0.090	0.003
Vio	0.55	0.00	0.57	0.006	0.004	0.000
Diad	0.81	0.03	0.85	0.055	0.041	0.006
Allo	0.76	0.00	0.85	0.016	0.010	-0.003
Dlato	0.41	0.00	0.44	0.010	0.007	0.001
Zea	0.62	0.00	0.62	0.010	0.007	0.001
Lut	0.068	0.00	0.30	0.003	0.002	-0.000
a_Caro	0.27	0.00	0.45	0.005	0.004	-0.001
B_Caro	0.88	0.00	0.92	0.009	0.006	0.001

Empirical Orthogonal Function

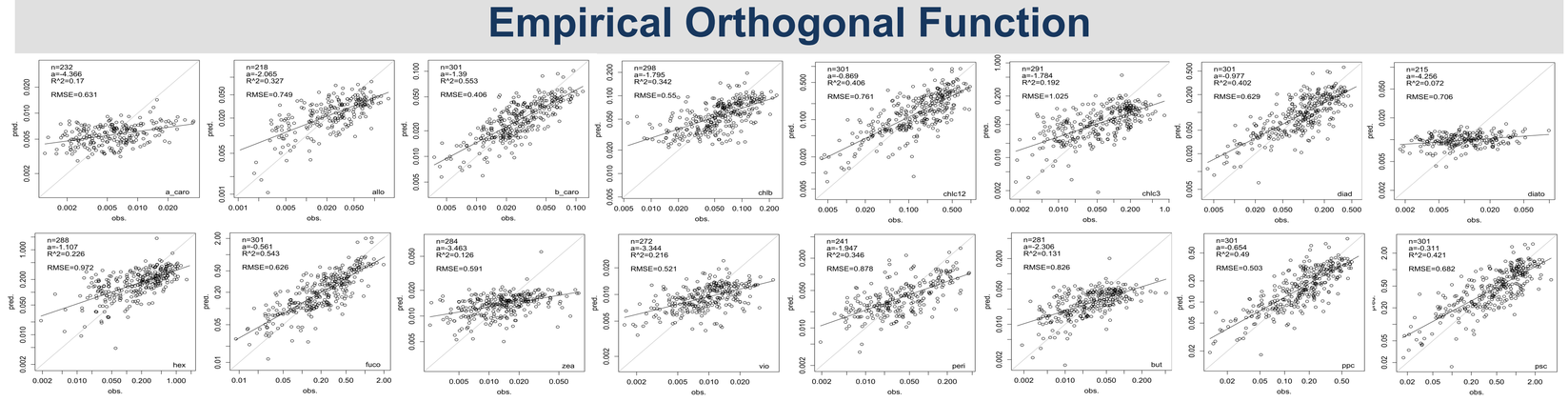

Outlook

1. Further consider the influence of package effect to particulate absorption spectra, to get more accurate predictions of pigment concentrations.
2. Different pigment concentration data will be used as input of CHEMTAX program to derive Phytoplankton Functional Types.

References:

Bracher, A., Taylor, M.H., Taylor, B., Dinter, T., Röttgers, R. and Steinmetz, F., 2014. Using empirical orthogonal functions derived from remote sensing reflectance for the prediction of concentrations of phytoplankton pigments. *Ocean Science Discussions*, *11*(5), pp.2073-2117.

Bricaud, A., Claustre, H., Ras, J. and Oubelkheir, K., 2004. Natural variability of phytoplanktonic absorption in oceanic waters: Influence of the size structure of algal populations. *Journal of Geophysical Research: Oceans*, *109*(C11).

Chase, A., Boss, E., Zaneveld, R., Bricaud, A., Claustre, H., Ras, J., Dall'Olmo, G. and Westberry, T.K., 2013. Decomposition of in situ particulate absorption spectra. *Methods in Oceanography*, *7*, pp.110-124.

Moisan, J.R., Moisan, T.A. and Linkswiler, M.A., 2011. An inverse modeling approach to estimating phytoplankton pigment concentrations from phytoplankton absorption spectra. *Journal of Geophysical Research: Oceans*, *116*(C9).

Röttgers, R., McKee, D., & Woźniak, S. B. (2013). Evaluation of scatter corrections for ac-9 absorption measurements in coastal waters. Methods in Oceanography, 7, 21-39.

Slade, W. H., Boss, E., Dall'Olmo, G., Langner, M. R., Loftin, J., Behrenfeld, M. J., Roesler, C. & Westberry, T. K. (2010). Underway and moored methods for improving accuracy in measurement of spectral particulate absorption and attenuation. Journal of Atmospheric and Oceanic Technology, 27(10), 1733-1746.

Sullivan, J. M., Twardowski, M. S., Zaneveld, J. R. V., Moore, C. M., Barnard, A. H., Donaghay, P. L., & Rhoades, B. (2006). Hyperspectral temperature and salt dependencies of absorption by water and heavy water in the 400-750 nm spectral range. Applied Optics, 45(21), 5294-5309.

Zaneveld, J. R. V., Kitchen, J. C., & Moore, C. C. (1994, October). Scattering error correction of reflecting-tube absorption meters. In Ocean Optics XII (pp. 44-55). International Society for Optics and Photonics.